RSC Advances

This is an *Accepted Manuscript*, which has been through the Royal Society of Chemistry peer review process and has been accepted for publication.

Accepted Manuscripts are published online shortly after acceptance, before technical editing, formatting and proof reading. Using this free service, authors can make their results available to the community, in citable form, before we publish the edited article. This *Accepted Manuscript* will be replaced by the edited, formatted and paginated article as soon as this is available.

You can find more information about *Accepted Manuscripts* in the Information for Authors.

Please note that technical editing may introduce minor changes to the text and/or graphics, which may alter content. The journal's standard Terms & Conditions and the Ethical guidelines still apply. In no event shall the Royal Society of Chemistry be held responsible for any errors or omissions in this *Accepted Manuscript* or any consequences arising from the use of any information it contains.

ROYAL SOCIETY OF CHEMISTRY

www.rsc.org/advances

Please do not adjust margins

RSC Advances

ARTICLE

Preparation of uniform poly(urea–siloxane) microspheres through precipitation polymerization

Received 00th January 20xx,
Accepted 00th January 20xx

DOI: 10.1039/x0xx00000x

www.rsc.org/

Shusheng Li,[a] Xiangzheng Kong[b*] and Shengyu Feng[a*]

A novel type of highly uniform polymer microspheres, poly(urea–siloxane) (PUSs) was prepared through the precipitation polymerization of 1,3-bis(3-aminopropyl)-1,1,3,3-tetramethyldisiloxane (APTMDS) with isophorone diisocyanate (IPDI) in H_2O–acetone mixed solvent. No additives such as surfactant and initiator were used. The effects of monomer ratios, H_2O/acetone ratios, and monomer concentrations on the yields and morphologies of the PUSs were investigated. Results indicated that PUSs sizes can be regulated from 2.14 μm to 7.11 μm by varying monomer ratios, monomer concentrations and H_2O/acetone ratios. Hydrogen bonds between polyurea units, polyurea and APTMDS moieties which were identified as the main effects of the products, endowed the materials with good elasticity. The structures and morphologies of the materials were characterized by FT–IR, NMR, and SEM, and the thermal properties were characterized by TGA and DSC analyses.

1. Introduction

Siloxane–containing polymers have been extensively studied, because of their interesting combination of properties, such as high backbone flexibility, low glass–transition temperature, low surface tension, excellent dielectric properties, and physiological inertness or biocompatibility.[1, 2] Among the diverse siloxane-containing polymers, poly(urea–siloxane) (PUSs) composites are of importance. They were usually synthesized through condensation polymerization of multifunctional isocyanates with amine modified siloxane.[3-5] Therefore, they have unique binary structure, as well as supramolecular organizations via intermolecular hydrogen bonding interactions.[5-7] The structure–morphology, excellent tensile and viscoelasticity associated with these had resulted in some applications as coatings,[8] biomaterials,[9] and modifiers for various polymers.[10] In the past decades, most reported studies were focused on bulk monoliths. As far as we know, controllable preparation of PUSs microspheres has not been explored at all. The problem, is that the incorporation of PDMS and polyurea (PU) segments into the morphologies causes great difference between their solubility parameters.[11]

Undoubtedly, polymeric spheres with micro– or macro–sizes possess larger surface areas and are more flexible than bulk materials.[12] Silicone colloidal spheres have been used as catalysts,[13] biosensors,[14-15] chromatography,[16] drugs carriers,[17] and supports of vaccines,[18] enzymes,[19] antigens.[20] Furthermore, they display an irreplaceable role in a number of material areas as they are finely dispersed in polymer matrices to improve their mechanical properties.[21]

Studies have been conducted on the fabrication of various types of polysiloxane spheres, namely polysiloxane spheres modified or coated by other species,[22-24] organic and inorganic particles modified or coated by polysiloxane,[25-27] and interpenetrating polysiloxane/polymer spheres.[28] However, these spheres were obtained by multistep process, in which silicone parts are often prepared by hydrolytic polycondensation of trialkoxysilanes or trichlorosilanes.[29, 30] Therefore, these particles are also named polysiloxanes. The polycondensation does not lead to polysiloxane elastomers but polysilsesquioxanes,[31-33] which most often have a rigid structure.

Fortuniak and Vilanova et al. obtained elastic polysiloxane particles through hydrosilylation or free radical emulsion polymerization.[34, 35] The particle sizes and monodispersion are uncontrollable for unavoidable adhesion between particles. The expensive and potentially inactivated noble catalyst is essential but hard to be removed in hydrosilylation.[27, 35] Lai et al. prepared particles with a polyurea core and a polysiloxane shell by the sol–gel process, in which triethoxysilane–functionalized polymers were made to react with 3-aminopropyltriethoxysilane and isocyanate (NCO)–ended prepolymers.[36] In this case, 3-aminopropyltriethoxysilane is used as coupling agent to form three–dimensional Si–O–Si reticulation that restricts chain segment movement, but another organic–inorganic hybrid system is formed.

The rigid or elastic particles described above were prepared by heterogeneous polymerizations. In those processes,

[a] Key Laboratory of Special Functionalal Aggregated Materials & Key Laboratory of Colloid and Interface Chemistry (Shandong University), Ministry of Education; School of Chemistry and Chemical Engineering, Shandong University, Jinan 250100, P. R. China. E-mail: fsy@sdu.edu.cn
[b] College of Chemistry and Chemical Engineering, University of Jinan, Jinan, 250022, P. R. China. E-mail: xzkong@ujn.edu.cn

RSC Advances Accepted Manuscript

surfactants or stabilizers along with vigorous stirring were needed.[34, 37] In many cases, trace residual surfactants or stabilizers induce adverse consequences in many applications, particularly in biological and medical fields.[38, 39] Precipitation polymerization without any surfactants or stabilizers is a probable alternative method for preparation of polymeric microspheres, which originated in free radical precipitation polymerization of different vinyl monomers in recent decades.[40, 41] However, it is difficult to use for PUSs preparation because of the different functional groups in isocyanates and vinyl monomers.

For the preparation of pure PU spheres, Kong et al. proposed a novel protocol via condensation step precipitation polymerization of isophorone diisocyanate (IPDI) with H_2O in acetone.[42] Dalmais et al. further obtained uniform–size core–shell spheres from IPDI and poly(dimethylsiloxane–amide) prepolymer using a microfluid– assisted method.[43] As far as we know, the preparation of PUSs microspheres with a convenient synthetic route has not been explored at all. Herein, we report the fabrication of novel PUSs by one step precipitation polymerization of IPDI with 1,3-bis(3-aminopropyl)-1,1,3,3-tetramethyldisiloxane (APTMDS) in H_2O–acetone mixed solvent, in which, microsphere sizes from 2.14 μm to 7.11 μm can be precisely controlled. Unlike the previously reported studies on polymeric particles, this process is carried out without any surfactants and energy–consuming stirring.

2. Experimental

2.1 Materials

IPDI was purchased from Aladdin and used as received unless otherwise stated. Acetone was supplied by Tianjin Fuyu Chemicals. APTMDS was obtained from Hangzhou Dadi Chemicals and used as received. H_2O was double–distilled in the laboratory.

2.2 Synthetic procedures

PUSs was prepared through one step process. A typical preparation of PUSs is described as follows. At 30 °C, 1.4 g of IPDI and 0.6 g of APTMDS were dissolved each in 34.3 g of acetone. The APTMDS acetone solution was slowly dropped into IPDI acetone solution with stirring, followed by the addition of H_2O. After 4 h, the mixtures were separated by a filter membrane with pore size of 0.45 μm and washed with acetonitrile. The final product, PUSs, was obtained after vacuum drying at 50 °C. The experiments were also done on changing IPDI/APTMDS weight ratios (from 0/10, to 1/9, and to 6/4), H_2O/acetone volume ratios (from 1/9 to 5/5), and different monomer concentrations (from 1.0 wt–% to 5.0 wt-%).

2.3 Analytical methods

The morphologies of PUSs were examined by scanning electron microscopy (SEM; Hitachi S-4800). Samples were coated with a fine gold layer (about 20 mm thick) using the ion coating JEOL JFC 1200 apparatus. The size (D_n) and size distribution (D_w/D_n) of PUSs were evaluated by counting about 100 microspheres on SEM images. The chemical structures of PUSs were characterized by Fourier transform infrared spectroscopy (FT–IR; Bruker TENSOR 27) within the range of 4000 cm^{-1} to 400 cm^{-1} working at 4 cm^{-1} resolution. Nuclear magnetic resonance (^1H NMR and ^{13}C NMR) spectroscopies were conducted with a Bruker AV300 spectrometer operating at 300 MHz. Monomers and PUSs samples were dissolved in DMSO–d. The thermal properties of PUSs were examined by thermogravity analysis (TGA) and differential scanning calorimetry (DSC). The curves of TGA and DSC were obtained by Mettler SDTA851, and the tests were performed from room temperature to 600 °C at the rate of 10 °C·min^{-1} under argon atmosphere.

3. Results and discussion

3.1 Design and synthesis

Fig. 1 illustrates our design and synthesis pathway of PUSs using IPDI and APTMDS as the monomers. Amino groups of siloxane monomer APTMDS react with excess IPDI to form isocyanate–terminated pre–polymers with soft segments (Si–O–Si), in which APTMDS dissolved in acetone and dropped into IPDI acetone solution is preferred. Then, –NCO groups in the pre–polymers and excess IPDI react with H_2O to form carbamic acid, an unstable intermediate which transforms into amines with the release of carbon dioxide. These amino groups, in turn, react with –NCO of the pre-polymer and IPDI, leading to rigid urea groups (-NH-CO-NH-) in the polymer chains.

Precipitation polymerizations started as homogeneous solution of monomer and solvents. This was confirmed by an initially clear and transparent solution, which also indicated that generated pre-polymers were dissolved in the system. The reaction mixture turned turbid, indicating that the propagating chains have grown beyond their solubility limit in the medium (critical molecular weight) and precipitated to form primary particles. The phase-separation of growing polymer chains was caused by enthalpic precipitation in cases of unfavourable polymer-solvent interactions, or entropic precipitation in cases where cross-linking prevents the polymer and solvent from freely mixing.[44] The first case was the main reason for non-cross-linked structure of PUSs. This was justified by further cross-linking degree tests, where the PUSs was easily dissolved in protic solvent, methanol and ethanol at reflux. The dramatic effect of hydrogen bonding on the morphology and properties of siloxane-urea segmented copolymers and network morphologies of PU units have been demonstrated by previous fundamental studies.[7, 45-47] The resulting nucleus aggregated into larger microspheres, which continued to grow by capturing other particles and newly formed polymer chains, or by absorption and monomer polymerization. The turbidity increase of the reaction system

RSC Advances Accepted Manuscript

 This journal is © The Royal Society of Chemistry 2015

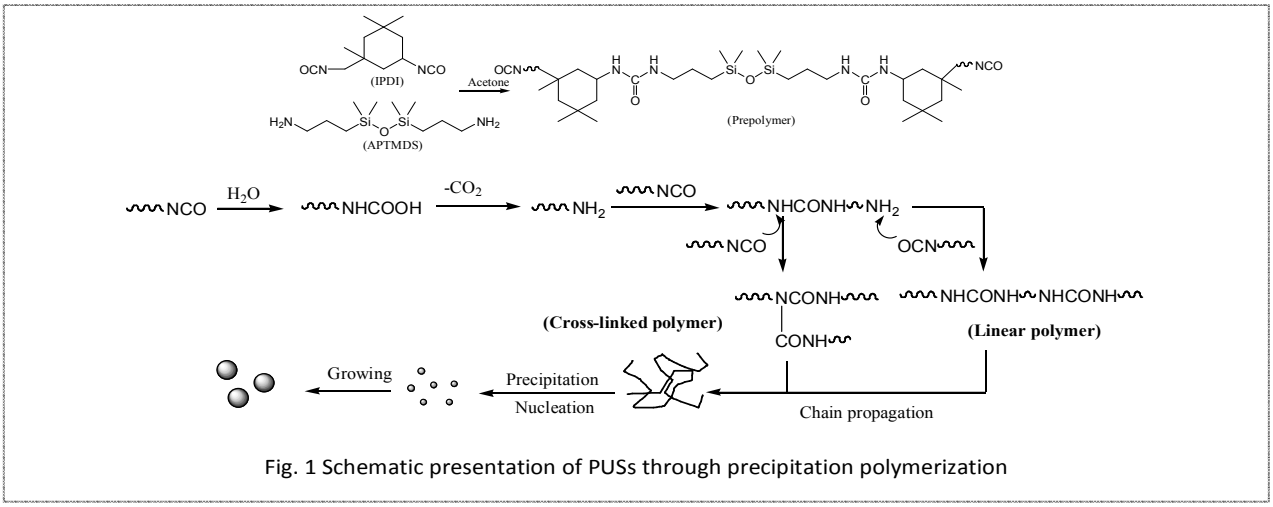

Fig. 1 Schematic presentation of PUSs through precipitation polymerization

indicated the growth of PUSs particles and a milk-like system was obtained.

3.2 Influence of IPDI/APTMDS ratios on formation of PUSs

In order to investigate the effect of the IPDI/APTMDS ratios on the yields and morphologies of PUSs, the experiments were carried out with varied weight of APTMDS from 0.0 wt-% to 60 wt-% in 3/7 H_2O–acetone mixed solvent. The results are listed in Table 1, and SEM images of PUSs are shown in Fig. 2.

Fig. 2 and Table 1 clearly show that PUSs of different sizes can be obtained by controlling monomer ratios. With increased APTMDS content, the sizes of PUSs gradually decreased from 6.11 μm to 2.49 μm. This may be caused by the decrease in surface energy. Microspheres with smaller sizes possess larger surface areas, which is thermodynamically unstable. The siloxane in the process can introduce desirable surface properties, with low surface energy as the most important. whether in non-aqueous or aqueous systems, silicones used as surface active agents can significantly reduce their surface tension to as low as 21 mN/m,[48] which benefited the formation of to PUSs with small size. Furthermore, particle sizes are related to the selected solvent in polymerization, as well as the hydrogen bonds index in the solvent. A polymer allows the forming the particles whose size could be larger than expected due to the presence of secondary forces.[49] Here, the content of polyurea groups and hydrogen bonds decreased along with IPDI content, which resulted in microspheres with smaller size. As shown in Table 1, the size distribution (D_w/D_n) of PUSs increased from 1.01 to 1.09 accordingly with increasing APTMDS from 0 wt-% to 50 wt-%. The rapid formation of PUSs nucleus should assume the main responsibility. The surplus particles formed in a short time intensified their collision, leading to a larger size distribution. The accelerated nuclei formation was visually displayed by turbid time. The precipitation of polymer chains and formation of primal particles accelerated with increased APTMDS, due to the hydrophobicity of Si-O-Si segments; thus, the turbid time (t_{turbid}) of the reaction system decreased. The yields of PUSs also clearly decreased slowly and their oligomers increased along with increased APTMDS from 0 wt-% to 50 wt-%. The more APTMDS reacted with IPDI, the less NCO groups were left. Harder contractions occurred between –NCO groups and newly formed NH_2 groups derived from –NCO group with H_2O. This inevitably reduced the polymer molecular weight and left more oligomers in the solvent. If NH_2/NCO was above 1 (S6P4) in molar ratio, then just a small (28.94 %) output was obtained. Undoubtedly, when no or little IPDI was involved, no chain growth occurred, and no PUSs was obtained. To summarize, the size of PUSs can be controlled by adjusting of APTMDS content (no more than 50 wt-%) in monomers at the expense of size distribution.

Table 1 Precipitation polymerization of PUSs for different APTMDS/IPDI weight ratios

Runs	APTMDS/IPDI (weight)	NH_2/NCO (moles)	*t_{turbid} (min)	D_n (μm)	D_w/D_n	Sphere Yields (%)	Oligomers (%)
*S0P10	0/10	0	48	6.11	1.01	60.36	30.28
S1P9	1/9	0.10	45	6.12	1.01	57.70	33.87
S2P8	2/8	0.22	33	6.04	1.02	53.73	36.03
S3P7	3/7	0.38	9	3.39	1.03	52.53	38.15
S4P6	4/6	0.59	7	2.79	1.06	51.14	42.99
S5P5	5/5	0.89	6	2.49	1.09	52.18	41.70
S6P4	6/4	1.34	0	/	/	28.94	63.43

* S0P10: S means APTMDS; P means IPDI; 0/10 means the mass ratio of APTMDS and IPDI.
* t_{turbid}: the minimum time for the precipitation polymerization system to begin to cloud.

RSC Advances Accepted Manuscript

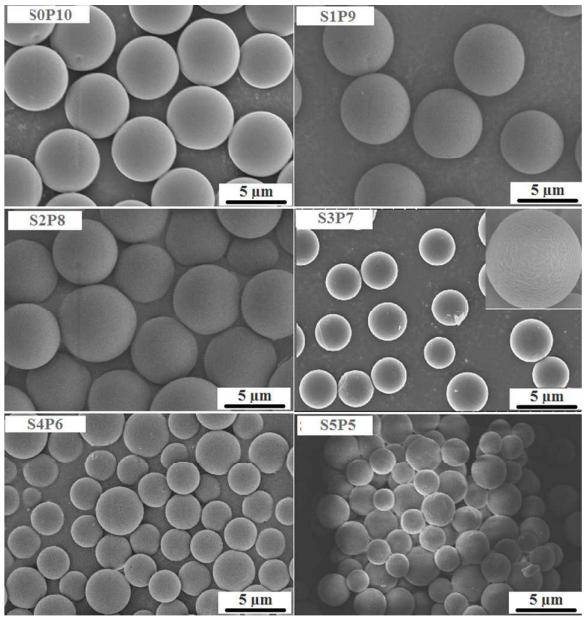

Fig.2 SEM images of PUSs obtained at different APTMDS/IPDI weight ratios

3.3 Influence of H_2O content on formation of PUSs

Selecting an appropriate solvent that enables the in-situ precipitation of forming PUSs microsphere into narrow disperse particles is important because the morphologies of the PUSs are greatly affected by solubility parameters.[50]

The impact of H_2O content on the formation and uniformity of PUSs was carried out with varied H_2O/acetone ratios in weight (1/9, 2/8, 3/7, and 4/6), keeping APTMDS/IPDI at 3/7 and the monomer constant at 2.0 wt-%. The obtained results are given in Table 2, and selected SEM images are shown in Fig. 3.

Table 2 and Fig. 3 clearly show that relatively uniform PUSs was formed when H_2O/acetone ratio was 3/7. With increased ratio to 4/6, the uniformity of PUSs decreased slightly from 1.03 to 1.04. This finding was due to the formation of more microspheres prompted by the reduced solubility of the oligomers in the polymerization medium. As aforementioned, the initially clear polymer solution in H_2O–acetone turned turbid as polymerization progressed. The turbidity time was sharply shortened from 75 min to 9 min with increased

Table 2 Precipitation polymerization of PUSs in H_2O-acetone mixed medium

H_2O–acetone (weight)	t_{turbid} (min)	D_n (μm)	D_w/D_n	Yields (%)	Oligomers (%)
1/9	75	2-6	/	31.09	60.38
2/8	40	2-6	/	34.87	52.13
3/7	9	3.39	1.03	52.53	43.15
4/6	1	2.14	1.04	66.50	24.96

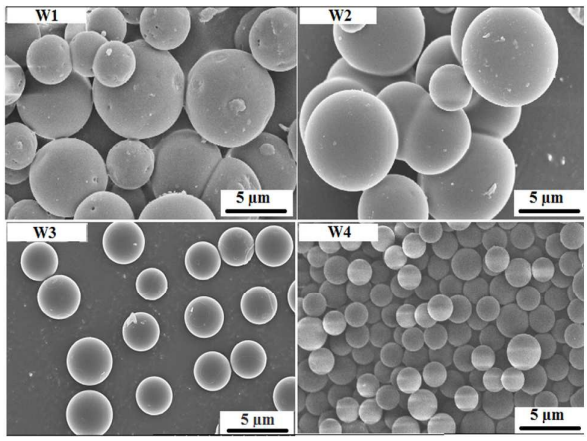

Fig.3 SEM images of the PUSs obtained at different H_2O content

H_2O/acetone ratio from 1/9 to 3/7, and the turbidity rapidly increased as the ratio reached 40 %. This advanced appearance of turbidity could be attributed either to an accelerated polymerization of pre–polymer with H_2O or to the reduced oligomer solubility. The earlier appearance of turbidity was mainly due to the latter rather than the former, because H_2O amount was much higher than –NCO groups of pre–polymer even at the lowest H_2O content. The subsequent reactions of –NCO groups with the newly formed amine were faster than the amine-yielding reaction of H_2O with –NCO groups, and therefore led to PUSs. PUSs was observed not to form if the reaction of -NCO group with H_2O instantaneously occurred. In this case, given that –NCO groups further reacting with amine groups were available shortly after the start of polymerization, amine-terminated IPDI monomers or oligomers remained in the system.

When H_2O/acetone ratios were 1/9, and 2/8, PUSs about 2 μm to 6 μm were obtained, whereas bigger ones were obtained at 3/7 and 4/6 H_2O/acetone ratios (2.24 and 2.10 μm, respectively). This may be caused by the aggregation of primal particles, similar to the size of PUSs obtained at 3/7 and 4/6 H_2O/acetone ratios. The aggregation that spontaneously occurred was perhaps due to their adhesive surface, which was related to solvent used in polymerization, and the aggregation led to serious coagulations and poor size distribution. H_2O in the mixed solvent plays two main roles. Firstly, as a part of mixed solvent, H_2O affect the morphologies of PUSs by changing the solubility parameters. Secondly, as a reactant, it react with –NCO to from NH_2 groups, which further react with –NCO to form growing polymer chains. Thus, If no was added in, the precipitation cannot conduct and no PUSs was obtained.

3.4 Influence of monomer concentration on formation of PUSs

In order to establish an appropriate protocol for the preparation of PUSs, we varied monomer concentrations from 1.0 wt-% to 6.0 wt-%, in H_2O–acetone mixed solvent of weight ratio 3/7. The obtained results are given in Table 3 and Fig. 4.

RSC Advances Accepted Manuscript

 This journal is © The Royal Society of Chemistry 2015

Fig. 4 shows that with increased monomer concentrations, the size of PUSs increased from 3.39 μm to 7.11 μm, and the size distribution decreased from 1.03 to 1.07 accordingly. This indicates that the sizes of PUSs could be controlled by varying monomer concentrations but at the expense of PUSs dispersity. The exasperated size distribution was caused by accelerated collision of the particles, which was induced by the rapid formation of a mass of nuclei particles at high monomer concentrations.

3.5 Structure characterization

3.5.1 FT-IR. The structures of synthesized PUSs were confirmed through FT-IR, ^{1}H NMR and ^{13}C NMR spectroscopy. The FT-IR spectra of IPDI and PUSs (S0P10 and S3P7) are displayed in Fig. 5. At absorption peaks of 2262 cm^{-1} in IPDI (Fig. 5 A), assigned stretching vibration of –N=C=O disappeared entirely in the PUSs (Fig. 5 B and Fig. 5 C), indicating that all –NCO groups of IPDI reacted. The strong stretching vibration peaks for N-H at 3360 cm^{-1}, C=O at 1654 cm^{-1}, C-N at 1240 cm^{-1} and plane banding vibration of N-H at 1550 cm^{-1}, confirm the formation of polyurea groups (-NH-CO-NH-).[51-53] The C=O and N–H observed at 1654 and 3360 cm^{-1}, respectively, suggest that the solid product was connected by disordered hydrogen bonding between the active hydrogen atoms of the two urea donor groups (N–H) in one urea molecule and an acceptor oxygen of the carbonyl group (C=O) in another urea molecule, but not the free urea (1690 cm^{-1}) or ordered hydrogen bonding (1630 cm^{-1}).[54, 55] Compared with S0P10 (Fig. 5 B), the obvious vibration absorption of Si–O–Si at 1053 cm^{-1}, and Si(CH$_3$)$_2$ at 847 and 790 cm^{-1}, confirm the successful introduction of the polysiloxane into PUSs.[11, 56] The absorptions at 2957 cm^{-1} and 2923 cm^{-1} are associated to stretching vibration of CH$_2$ and CH$_3$ respectively.

Table 3. Precipitation polymerization of PUSs at varied monomer concentrations

Monomer (wt-%)	D_n (μm)	D_n/D_w	Yields (%)	Oligomers (%)
2.0	3.39	1.03	52.53	43.15
3.0	4.24	1.04	56.84	40.13
4.0	4.51	1.06	60.19	34.57
5.0	6.58	1.06	66.51	26.96
6.0	7.11	1.07	70.22	24.59

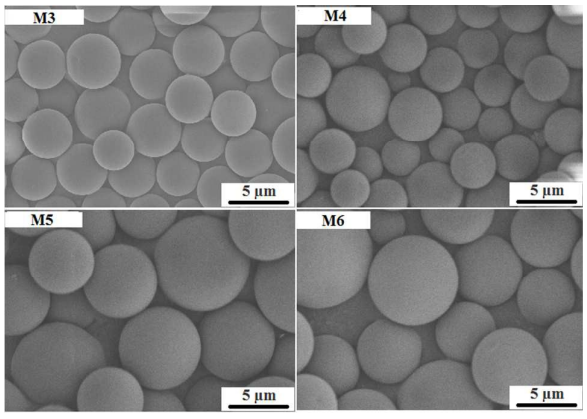

Fig. 4 SEM images of the microspheres obtained from precipitation step polymerization with varied monomer concentrations

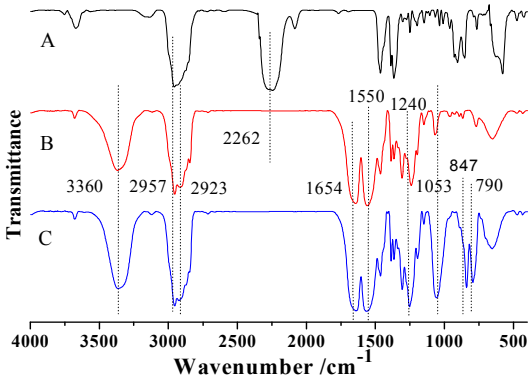

Fig.5 FT-IR spectra of IPDI (A), S0P10 (B), and S3P7 (C).

3.5.2 ^{1}H NMR. The ^{1}H NMR of monomers (APTDMS, IPDI) and PUSs (P7S3) are shown in Fig. 6. The resonance peaks of –Si-**CH$_3$**, –Si-**CH$_2$**–, and –Si-CH$_2$-**CH$_2$**– at 0.06, 0.52, and 1.44 ppm respectively, are easy to distinguish in APTDMS moiety (H$_1$, H$_2$, and H$_3$ in Fig. 6 A), and S3P7 (H$_{17}$, H$_{16}$, and H$_{15}$ in Fig 6 C), thereby confirming the presence of alkylsilane groups in PUSs.[57] The peaks at range of 0.9 ppm to 1.1 ppm, belonging to aliphatic ring carbon of IPDI (Fig. 6 B), appeared in S3P7 (Fig. 6 C), which confirms that IPDI became a part of S3P7. In ^{1}H NMR spectra of S3P7, the relative areas of the signals at 5.83 and 3.32 ppm (Fig. 6 C) assigned to –NH–CO–NH– and –CH$_2$–NH–, respectively, confirms the presence of urea group.[58] In addition, the peak of NH$_2$ at 1.14 ppm in APTDMS (Fig. 6 A) disappeared in S3P7 (Fig. 6 C). The signal assigned to the methylene groups linked to NH$_2$ groups, whose position shifts from 2.65 ppm in APTDMS to 3.32 ppm in S3P7, confirms the chemical linkage between APTDMS and IPDI.

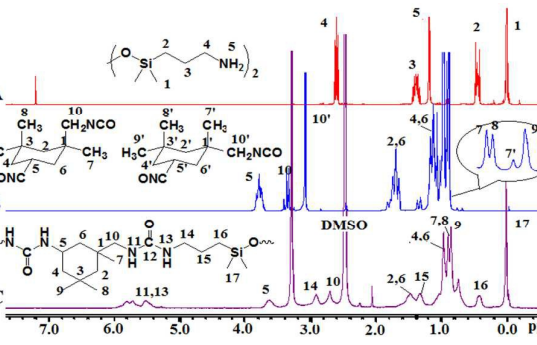

Fig. 6 ^{1}H NMR spectra of APTDMS (A), IPDI (B), P7S3 (C)

RSC Advances Accepted Manuscript

3.5.3 ^{13}C NMR. ^{13}C NMR tests on PUSs (P7S3) were also carried out along with APTDMS and IPDI. All the spectra are displayed in Fig. 7. ^{13}C NMR (Fig. 7 B) spectra of IPDI indicated its mixed characters similar to its ^{1}H NMR (Fig. 6 B), because IPDI is composed of two stereisomer, cis-isomer (75%) and trans-isomer (25%). The characteristic peaks of –Si-**CH_3** –Si-**CH_2**–, and –Si-CH_2-**CH_2**– at 0.00, 14.73, and 27.02 ppm in APTDMS also appear in S3P7, indicating the existence of alkylsilane groups in the PUSs.[31] The peaks at range of 20 ppm to 50 ppm in S3P7 (Fig. 7 C), belong to aliphatic ring carbon of IPDI (Fig. 7 B), confirms the presence of IPDI segment in S3P7. The peak of C_4 at 44.72 ppm in APTDMS (Fig. 7 A) and C_5, C_{10} at range of 50 ppm to 60 ppm in IPDI (Fig. 7 B) do not appeared at original position in S3P7, confirming the reaction between NH_2 and -NCO group.

3.6 PUSs solubility test

In order to study the properties of cross-linking in PUSs, the solubility of PUSs were studied by taking S3P7 as a typical representative. The APTMDS-free PUSs (S0P10) was hardly dissolved in protic solvents (methanol and ethanol) and most nonprotic solvents (dichloromethane, trichloromethane and acetonitrile) except hot DMSO. However, once the monomer ratio of APTMDS/IPDI was increased to 3/7, PUSs (S3P7) was easily dissolved in protic solvents but not in the nonprotic ones. This observation supports the conclusion that the physical cross-linking of hydrogen bonding between polyurea units that exist in the PUSs is a result of PUSs morphologies, which supply the cumulative cohesive energy in the PUSs. In addition, the high electronegativity of nitrogen atom in the urethane or urea moiety withdraws N–H bonded electrons and develops partial positive charge on the hydrogen, thereby forming hydrogen bonding with oxygen atom.[59] In all cases, the hydrogen atom of the N–H group in the urethane or urea linkages is the donor proton, while the acceptor group is the carbonyl of the imide groups, urethane's C=O, or urea's C=O. The hydrogen bonding interaction produces physical crosslinks, thereby reinforcing the PU matrix; and increases strength and stiffness.[52] Thus, the PUSs should process drastic enhanced mechanical and tensile properties. This is true in the case of siloxane polymers because the constitutive ($OSi[Me]_2$) units do not permit the establishment of strong interactions

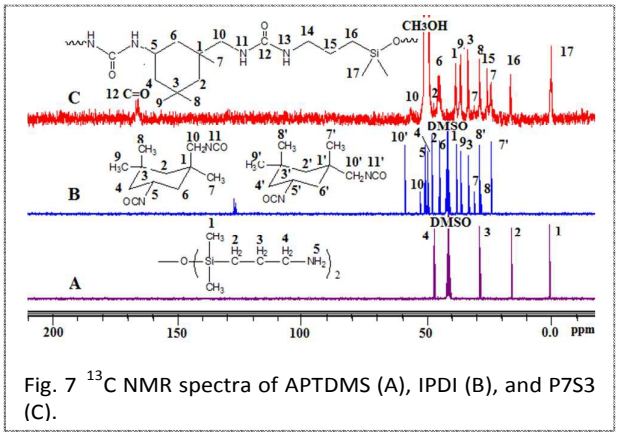

Fig. 7 ^{13}C NMR spectra of APTDMS (A), IPDI (B), and P7S3 (C).

Table 4 Solubility behavior of synthesized PUSs

Solvents	S0P10	S1P9	S2P8	S3P7	S4P6	S5P5
DMSO	±	±	±	±	±	±
CH_3OH	-	±	±	+	+	+
CH_3CH_2OH	-	±	±	+	+	+
CH_3CN	-	-	-	-	-	-
CH_2Cl_2	-	-	-	-	-	-
$CHCl_3$	-	-	-	-	-	-

(+): Soluble at room temperature. (±): Partially soluble with warming. (-): Insoluble.

with the other polymer or units, and a small content of the polysiloxane allows a reduction in the interfacial tension. Therefore, a great APTMDS leads to easier dissolution of PUSs in protic solvents.

3.7 Thermal properties of PUSs

TGA and DSC tests were used to evaluate the thermal resistance of PUSs. Results are shown in Fig.8.

The similar curves of TGA and DSC for all samples in Fig.8 indicated their similar molecular structures. Taking TGA curve of S3P7 as an example, it has an appreciable weight loss of 5% at about 310.6 °C ($T_{5\%}$, initial temperature of degradation), 50% at 352.1 °C ($T_{1/2}$, temperature of 50 % weight loss), and, 90% at 402.3 °C ($T_{90\%}$, temperature of 90 % weight loss). On the DSC curve, an obvious degradation endothermic peak was obtained at 357.5 °C (T_d). The weight loss and endothermic peak was caused by the decomposition of urea units. Several literature have shown that the decomposition of poly(urea-silicone) or poly(urethane-silicone) copolymers is in a two-way step, related to hard segments and soft segments.[60] Here, only

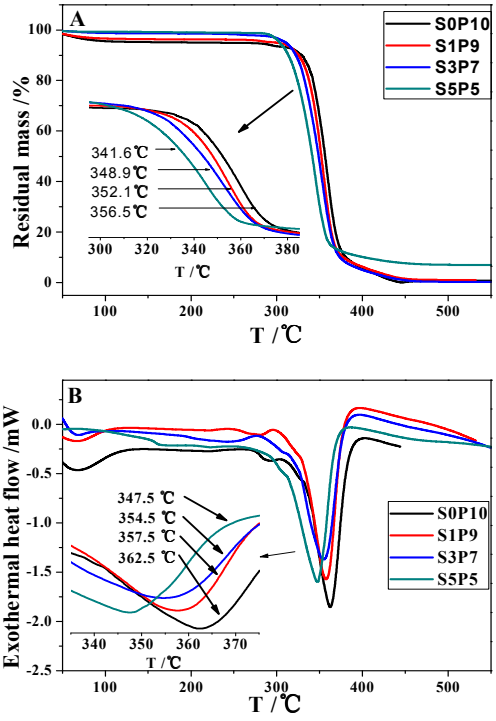

Fig. 8 TGA (A) and DSC (B) curves of PUSs

RSC Advances Accepted Manuscript

 This journal is © The Royal Society of Chemistry 2015

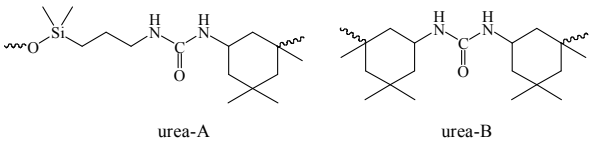

Fig. 9 Two types urea groups existing in PUSs: urea-A and urea-B

one decomposition step was observed due to the highly incorporated structure of PUSs. That is to say, no obvious hard and soft segments were present in the PUSs, but alternate structures of short siloxane and urea units were observed.

With the content of siloxane in PUSs samples (S0P10, S1P9, S3P7, and S5P5) increased from 0% to 50%, the $T_{1/2}$ and T_d decreased from 356.5 °C to 341.6 °C and from 362.5 °C to 347.5 °C respectively. The initial degradations of the copolymers occurred at the urea group (-NH-CO-NH-). However, examining the structures of PUSs, two types of urea were distinguished: urea-A and urea-B (Fig. 9). Therefore, the initial degradation of PUSs may occur at urea-A and/or at urea-B. At the range of 300 °C to 340 °C of TGA curves, the samples displayed different degradation rates (the weight loss percentage per minute, %/min). As the content of urea-A in PUSs increased, the degradation rates increased accordingly: 2.7 %/min of S0P10, 4.5 %·min^{-1} of S1P9, 7.2 %·min^{-1} of S3P7, and 10.7 %·min^{-1} of S5P5. The degradation of polyurethane and polyurea segments is a depolymerization process.[60] Thus, in this case, urea-A degraded to form $PDMS_2$ and IPDI fragments, while the degradation of urea-B possibly formed IPDI fragment only. The $PDMS_2$ had higher volatility than IPDI, and had most effect in the region. In common studied poly(urea-silicone) or poly(urethane-silicone) copolymers, a high temperature is need to break Si-O-Si and great heat resistance was exhibited when long polysiloxane involved in. However in PUSs, siloxane parts are so short to provide heat resistance and signification change of PUSs were obtained in DSC and TGA. In spite of this, all samples of PUSs can be assumed to have excellent heat resistance at 300 °C in an inert atmosphere.

4. Conclusions

PUSs with uniform size and clear surface, were first prepared through precipitation step polymerization of isocyanate-end capped siloxane in H_2O–acetone mixed solvent without any additives. Selecting a H_2O–acetone mixed solvent that enables the in–suit precipitation of forming PUSs into narrow disperse particles is important. PUSs sizes can be controlled from 2.14 μm to 7.11 μm by changing monomer ratios and concentrations and H_2O/acetone ratios. FTIR and NMR spectra showed the successful introduction of polyurea groups (-NH-CO-NH-) and polysiloxane moiety into PUSs. The solubility test supports the conclusion that a physical cross-linking of hydrogen bonds between polyurea units, polyurea and APTMDS moiety existing in the PUSs is mainly the effect of these PUSs morphologies. TGA and DSC analysis of the PUSs indicated that all samples exhibit excellent thermal resistance at 300 °C.

Acknowledgements

This work was financially supported by the National Natural Science Foundation of China (No.21274080) and Special Fund for Shandong Independent Innovation and Achievements transformation（No.2014ZZCX01101）

References

1. E. Pouget, J. Tonnar, P. Lucas, P. Lacroix-Desmazes, F. o. Ganachaud and B. Boutevin, *Chem. Rev.*, 2009, **110**, 1233-1277.
2. E. Yilgör and I. Yilgör, *Prog. Polym. Sci.*, 2014, **39**, 1165-1195.
3. L.-T. T. Nguyen, X. K. D. Hillewaere, R. F. A. Teixeira, O. van den Berg and F. E. Du Prez, *Polym. Chem.*, 2015, **6**, 1159-1170.
4. E. Yilgor, T. Eynur, C. Kosak, S. Bilgin, I. Yilgor, O. Malay, Y. Menceloglu and G. L. Wilkes, *Polymer*, 2011, **52**, 4189-4198.
5. J. C. Johnson, N. D. Wanasekara and L. T. J. Korley, *J. Mater. Chem. B*, 2014, **2**, 2554.
6. E. Yilgor, G. Ekin Atilla, A. Ekin, P. Kurt and I. Yilgor, *Polymer*, 2003, **44**, 7787-7793.
7. A. Rekondo, M. J. Fernández-Berridi and L. Irusta, *Eur. Polym. J.*, 2006, **42**, 2069-2080.
8. M. Lejars, A. Margaillan and C. Bressy, *Chem. Rev.*, 2012, **112**, 4347-4390.
9. T. Choi, K. A. Masser, E. Moore, J. Weksler, A. Padsalgikar and J. Runt, *J. Polym. Sci. Part B: Polym. Phys.*, 2011, **49**, 865-872.
10. E. Yilgör, İ. Yilgör and S. Süzer, *Polymer*, 2003, **44**, 7271-7279.
11. M. V. Pergal, J. V. Džunuzović, R. Poręba, S. Ostojić, A. Radulović and M. Špírková, *Prog. Org. Coat.*, 2013, **76**, 743-756.
12. K. E. Sapsford, W. R. Algar, L. Berti, K. B. Gemmill, B. J. Casey, E. Oh, M. H. Stewart and I. L. Medintz, *Chem. Rev.*, 2013, **113**, 1904-2074.
13. B. Heurtefeu, C. Bouilhac, É. Cloutet, D. Taton, A. Deffieux and H. Cramail, *Prog. Polym. Sci.*, 2011, **36**, 89-126.
14. D. Giaume, M. Poggi, D. Casanova, G. Mialon, A. Alexandrou, T. Gacoin, and J.-P. Boilot, *Langmuir*, 2008, **24**, 11018-11026.
15. F. Li, J. Li and S. Zhang, *Talanta*, 2008, **74**, 1247-1255.
16. M. Buchmeiser, R. , *J. Chromatogs. A*, 2001, **918**, 233-266.
17. Y. Zhang and D. Rochefort, *J. microencapsulation*, 2012, **29**, 636-649.
18. R. Asasutjarit, S. I. Lorenzen, S. Sirivichayakul, K. Ruxrungtham, U. Ruktanonchai and G. C. Ritthidej, *Pharm. Res.*, 2007, **24**, 1098-1107.

RSC Advances Accepted Manuscript

19.A. Durdureanu-Angheluta, M.-E. Ignat, S. S. Maier, L. Pricop, A. Coroaba, A. Fifere, M. Pinteala and A. Chiriac, *Appl. Surf. Sci.*, 2014, **292**, 898-905.
20.M. Zhao, Y. Xie, C. Deng and X. Zhang, *J. Chromatogs. A*, 2014, **1357**, 182-193.
21.X. Qian, B. Yu, C. Bao, L. Song, B. Wang, W. Xing, Y. Hu and R. K. K. Yuen, *J. Mater. Chem. A*, 2013, **1**, 9827.
22.P. K. Roy, N. Iqbal, D. Kumar and C. Rajagopal, *Polym. Bull.*, 2014, **71**, 2733–2748.
23.C. I. Zoldesi, C. A. v. Walree and A. Imhof, *Langmuir*, 2006, **22**, 4343-4352.
24.M. W. Patchan, B. W. Fuller, L. M. Baird, P. K. Gong, E. C. Walter, B. J. Vidmar, I. Kyei, Z. Xia and J. J. Benkoski, *ACS Appl. Mater. Interf.*, 2015, **7**, 7315-7323.
25.S.-L. Gong, Z.-J. Yu, L.-Z. Meng, L. Hu and Y.-B. He, *J. Appl. Polym. Sci.*, 2004, **93**, 637-643.
26.X. Lu and Z. Xin, *Colloid Polym. Sci.*, 2006, **285**, 599-604.
27.W. Fortuniak, S. Slomkowski, J. Chojnowski, J. Kurjata, A. Tracz and U. Mizerska, *Colloid Polym Sci*, 2013, **291**, 725-733.
28.R. K. Nagarale, J. M. Lee and W. Shin, *Electrochim. Acta*, 2009, **54**, 6508-6514.
29.J. Hu, Y. Zhou, M. He and X. Yang, *Opt. Mater.*, 2013, **36**, 271-277.
30.H. Zou, S. Wu and J. Shen, *Chem. Rev.*, 2008, **108**, 3893-2957.
31.J. P. Randall, M. A. B. Meador and S. C. Jana, *J. Mater. Chem. A*, 2013, **1**, 6642.
32.B. Liu, Z. Sun, J. Wu and S. Huang, *RSC Advances*, 2014, **4**, 50249-50253.
33.Z. Ren, Z. Chen, W. Fu, R. Zhang, F. Shen, F. Wang, Y. Ma and S. Yan, *J. Mater. Chem.*, 2011, **21**, 11306.
34.W. Fortuniak, J. Chojnowski, S. Slomkowski, P. Pospiech and J. Kurjata, *Polymer*, 2013, **54**, 3156-3165.
35.N. Vilanova, C. Solans and C. Rodriguez-Abreu, *Langmuir*, 2013, **29**, 15414-15422.
36.X. Lai, X. Li, L. Wang and Y. Shen, *Polym. Bul.*, 2010, **65**, 45-57.
37.Y. Hou, A. R. Matthews, A. M. Smitherman, A. S. Bulick, M. S. Hahn, H. Hou, A. Han and M. A. Grunlan, *Biomaterials*, 2008, **29**, 3175-3184.
38.T. Ivankovic and J. Hrenovic, *Arhiv za higijenu rada i toksikologiju*, 2010, **61**, 95-110.
39.E. Liwarska-Bizukojc, K. Miksch, A. Malachowska-Jutsz and J. Kalka, *Chemosphere*, 2005, **58**, 1249-1253.
40.X. Z. Kong, X. L. Gu, X. Zhu and L. Zhang, *Macromol. Rapid commu.*, 2009, **30**, 909-914.
41.H. Jiang, H. Chen, G. Zong, X. Liu, Y. Liang and Z. Tan, *Polym. Adv. Technol.*, 2011, **22**, 2096-2103.
42.X. Jiang, X. Z. Kong and X. Zhu, *J. Polym. Sci. Part A: Polym. Chem.*, 2011, **49**, 4492-4497.
43.A. Dalmais, C. A. Serra, Z. Chang, M. Bouquey and R. Muller, *Macromol. Mater. Eng.*, 2014, **299**, 698-706.
44.J. S. Downey, R. S. Frank, W. H. Li and H. D. H. Stöver, *Macromolecules*, 1999, **32**, 2838-2844.
45.J. P. Sheth, D. B. Klinedinst, G. L. Wilkes, I. Yilgor and E. Yilgor, *Polymer*, 2005, **46**, 7317-7322.
46.J. P. Sheth, A. Aneja, G. L. Wilkes, E. Yilgor, G. E. Atilla, I. Yilgor and F. L. Beyer, *Polymer*, 2004, **45**, 6919-6932.
47.S. Sami, E. Yildirim, M. Yurtsever, E. Yurtsever, E. Yilgor, I. Yilgor and G. L. Wilkes, *Polymer*, 2014, **55**, 4563-4576.
48.S.-Q. Wei, Y.-P. Bai and L. Shao, *Eur. Polym. J.*, 2008, **44**, 2728-2736.
49.S. A. Jenekhe, *Science*, 1999, **283**, 372-375.
50.E. C. C. Goh and H. D. H. Stvver, *Macromolecules*, 2002, **35**, 9983-9989.
51.E. Maya-Visuet, T. Gao, M. Soucek and H. Castaneda, *Prog. Org. Coat.*, 2015, **83**, 36-46.
52.L. Feng and J. O. Iroh, *Eur. Polym. J.*, 2013, **49**, 1811-1822.
53.G. Wu, J. An, D. Sun, X. Tang, Y. Xiang and J. Yang, *J. Mate. Chem. A*, 2014, **2**, 11614.
54.J. Mattia and P. Painter, *Macromolecules*, 2007, **40**, 1546-1554.
55.J. Shang, S. Liu, X. Ma, L. Lu and Y. Deng, *Green Chem.*, 2012, **14**, 2899.
56.L. F. Wang, Q. .Ji, T. E. Glass, T. C. Ward, J. E. McGrath, M. Mugglic, G. Burnsd and U. Sorathia, *Polymer*, 2000, **41**.
57.A. Halim, Q. Fu, Q. Yong, P. A. Gurr, S. E. Kentish and G. G. Qiao, *J. Mater. Chem. A*, 2014, **2**, 4999.
58.R. Chakraborty and M. D. Soucek, *Macromol. Chem. Phys.*, 2008, **209**, 604-614.
59.M. Ionescu, *Rapra Technology, Ltd, Shrewsbury, Shropshire, UK*, 2005.
60.F.-S. Chuang, H.-Y. Tsi, J.-D. Chow, W.-C. Tsen, Y.-C. Shu and S.-C. Jang, *Polym. Degrad. Stab.*, 2008, **93**, 1753-1761.

RSC Advances Accepted Manuscript

 This journal is © The Royal Society of Chemistry 2015

RSC Advances Accepted Manuscript